Structure, magnetic ordering, and Kondo effect in $(Ce_{1-x}Nd_x)_3Al$

Lingwei Li,[1] Ryoichi Yamagata,[1] Katsuhiko Nishimura,[1] and Hitoshi Yamaoka[2]
[1]*Graduate School of Science and Engineering, University of Toyama, Toyama 930-8555, Japan*
[2]*Harima Institute, The Institute of Physical and Chemical Research (RIKEN), Sayo, Hyogo 679-5148, Japan*
(Received 26 June 2009; revised manuscript received 7 October 2009; published 30 October 2009)

A systematic study for $(Ce_{1-x}Nd_x)_3Al$ ($x=0-1.0$) compounds has been performed by measuring lattice parameters, electrical resistivity, magnetization, and specific heat. All samples exhibit the hexagonal crystal structure at room temperature. The lattice parameters and unit-cell volume decrease monotonically with increasing Nd content (x). An obvious hysteresis in temperature dependence of resistivity, which was attributed to the crystal structural phase transition, is found at $x \leq 0.3$. The low-temperature resistivity shows $\log T$ dependence, suggesting the Kondo effect at $x \leq 0.3$. The Néel temperature and structural transition temperature (T_S) decrease with increasing x, T_S merges with the antiferromagnetic (AFM) transition, and the Curie temperature increases linearly with increasing x at $x \geq 0.2$. Thus $x \sim 0.2$ is a critical point where the ferromagnetic order and Kondo effect compete at low temperature. The effective magnetic moments μ_{eff} almost linearly decrease with increasing x and agree with the estimation assuming Nd^{3+} and Ce^{3+} states, indicating that the change in the electronic structures of Nd and Ce ions in the ground states is very small in the entire range. The characteristic temperature T_0 which was obtained by the fitting of Rajan's curve decreases with increasing x at $x \leq 0.15$, i.e., a small fraction of Nd content strongly dilute the Kondo effect as well as AFM order.

DOI: 10.1103/PhysRevB.80.134429 PACS number(s): 72.15.Qm, 75.30.Mb, 61.66.Dk, 75.40.−s

I. INTRODUCTION

Cerium-based intermetallic compounds have been extensively studied experimentally and theoretically due to their interesting physical properties such as Kondo effect, heavy fermion behavior, valence fluctuation, superconductivity, and magnetic properties.[1–9] It is well known that the anomalous physical properties of Ce-based dense Kondo systems are considered to arise from the strong hybridization between localized $4f$ electrons and the conduction electrons. It has been shown that under the hybridization there is a competition between the Ruderman-Kittel-Kasuya-Yosida (RKKY) interaction and the Kondo effect which have great influence on the physical properties of materials.

Among Ce-Al compounds, R_3Al (R=Ce, La, Pr, and Nd) system has attracted much attention. The R_3Al is crystallized in the hexagonal Ni_3Sn structure with the space group of $P6/mmc$ at room temperature.[10] Ce_3Al is known to be a heavy fermion with $\gamma \sim 100$ mJ/K^2/Ce mol. Ce_3Al shows a crystal phase transition around 110 K, single-impurity Kondo effect around 20 K, and an antiferromagnetic transition at 2.8 K as well as the valence fluctuation of Ce below 110 K.[11–17] Recent high-pressure study for Ce_3Al shows the pressure-induced Kondo volume collapse and $4f$ electron delocalization.[18] Chen *et al.*[19] found the size-induced phase transition from magnetic ordering to Kondo behavior in Ce_3Al. La_3Al shows a crystal phase and a superconducting transition around 55 and 6 K, respectively.[16,17,20] Pr_3Al shows two magnetic phase transitions: a ferromagnetic (FM) order at 4.8 K and an antiferromagnetic (AFM) order at 10 K.[21] Recently Fukuhara *et al.*[22] reported the specific-heat and transport properties of Nd_3Al which shows a ferromagnetic order below 74 K. The lattice parameters, resistivity, susceptibility, specific heat, and the thermal electrical power in a La-substituted system of $(Ce_{1-x}La_x)_3Al$ ($x=0-1$) (Refs. 12, 14, 16, 17, and 23) and a Y-substituted system of $(Ce_{1-x}Y_x)_3Al$ ($x=0-0.2$) (Refs. 12 and 16) for Ce_3Al had been studied. La substitution for Ce site in Ce_3Al causes the increase in the volume, suppression of AFM order, and decrease in the Kondo temperature. In La-rich samples superconductivity is observed. Thus Nd substitution to Ce site in Ce_3Al system may be another typical candidate to study the phase transition from Kondo system to magnetic ordered state because of the strong magnetic property of Nd_3Al. It is also physically interesting to observe the effect of Nd substitution on the competition between the Kondo effect and RKKY interaction in Ce-rich side of $(Ce_{1-x}Nd_x)_3Al$. Furthermore, we could see the effect of $4f$ electrons of substituted atoms on Ce in Ce_3Al because La^{3+} have no $4f$ electrons in $(Ce_{1-x}La_x)_3Al$ while Nd^{3+} corresponds to $4f^3$ in $(Ce_{1-x}Nd_x)_3Al$. In this paper we report a systematic study of crystal structure, magnetic and thermodynamic properties in $(Ce_{1-x}Nd_x)_3Al$ system, and the phase diagram is determined. Our results show that the effect of the change in the volume on the properties of the Kondo system in the $(Ce_{1-x}Nd_x)_3Al$ is very different from the $(Ce_{1-x}La_x)_3Al$ system.

II. EXPERIMENTS

Polycrystalline samples of $(Ce_{1-x}Nd_x)_3Al$ ($x=0-1.0$) were prepared by an arc melting method using a tungsten electrode under an argon atmosphere. First, we melted the stoichiometric amounts of Nd, Ce, and Al on a water-cooled copper hearth. The sample was melted more than six times for homogeneity. The total weight loss of the sample obtained by this method was less than 0.5%. Then the samples were annealed for one week at 773 K and followed by three weeks at 473 K in evacuated quartz tubes to obtain the hexagonal phase.[16] All the samples were prepared under identical conditions. The crystal structures were determined by x-ray diffraction (XRD) experiment. The samples were cut into rectangular pieces for measurements of electrical resis-

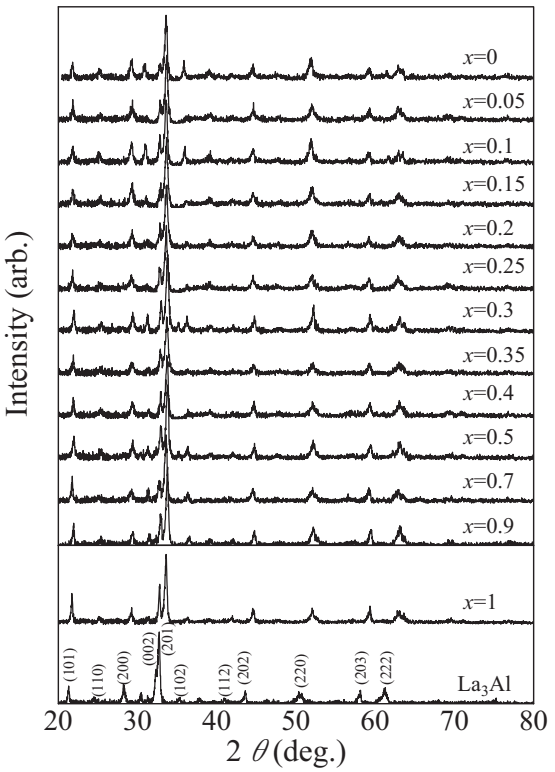

FIG. 1. X-ray diffraction patterns in $(Ce_{1-x}Nd_x)_3Al$ at room temperature.

tivity, which were carried out using a standard four-probe technique in the temperature range from 1.8 to 280 K. Magnetization measurement was carried out using a superconducting quantum interference device (Quantum Design, magnetic property measurement system) in the temperature range from 2 to 300 K. Specific-heat measurements were carried out by the adiabatic heat relaxation method in the temperature range from 2 to 200 K using physical property measurement system (PPMS-9) made by Quantum Design.

III. RESULTS AND DISCUSSION

X-ray diffraction was performed on all the samples at room temperature and the results are shown in Fig. 1. No impurity peak was found within the experiment errors; all the samples are single phased with Ni_3Sn-type hexagonal crystal structure at room temperature. The results suggest that the $(Ce_{1-x}Nd_x)_3Al$ ($x=0-1.0$) is a complete pseudobinary solid solution. The lattice parameters at room temperature are deduced by the least-squares method from the XRD data as shown in Fig. 2. The results of Ce_3Al and Nd_3Al alloys are in good agreement with previously measured values.[12,17,22] The lattice parameter does not change along c axis as a function of x but it does along a and b axes, resulting that the volume monotonically decreases with increasing x. In $(Ce_{1-x}La_x)_3Al$ the volume (V) increases largely with increasing La concentration by $\Delta V/V \sim 8\%$, where ΔV is change in the volume, as well as the increase in Y concentration in $(Ce_{1-x}Y_x)_3Al$ system.[12,16,17] $\Delta V/V$ is, however, less than $\sim 1.5\%$ for $(Ce_{1-x}Nd_x)_3Al$ and increase in the Nd concentration causes

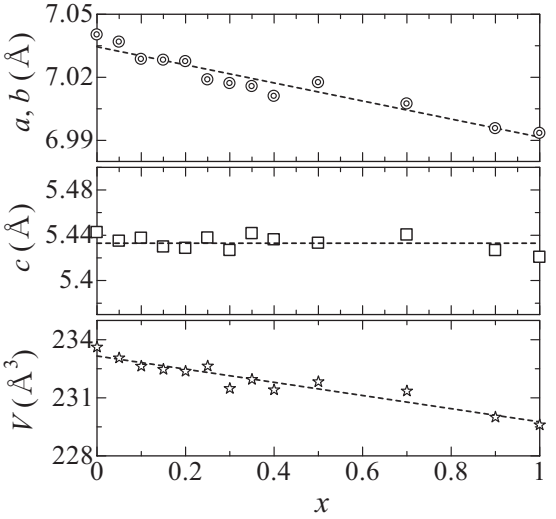

FIG. 2. Lattice parameters a and c as well as unit-cell volume V as a function of x in $(Ce_{1-x}Nd_x)_3Al$ at room temperature.

the decrease in volume. Figure 3(a) shows the temperature dependence of susceptibility (χ) at temperature range from 2 to 300 K in an external field $H=1$ kOe. Magnetic phase transition from paramagnetic (PM) to AFM is observed for Ce-rich samples at $x \leq 0.1$ and the transition temperature T_N decreases with decreasing x very rapidly. In contrast, the FM transition is observed for Nd-rich samples clearly and the Curie temperature (T_C) gradually increases with increasing Nd content x.

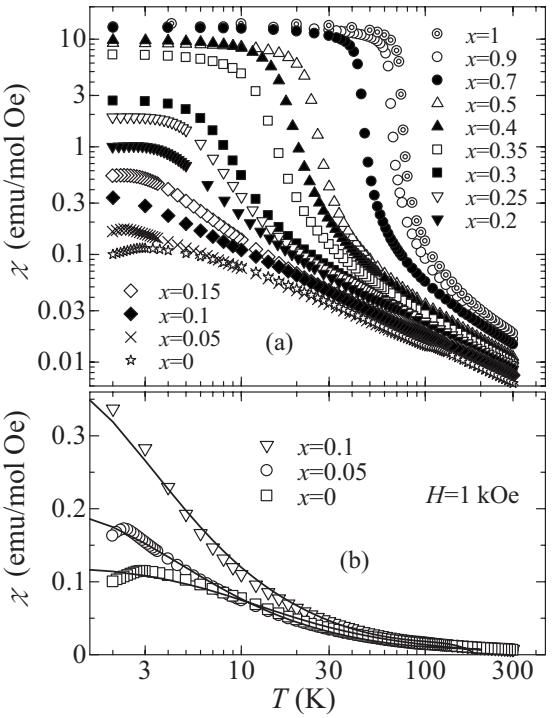

FIG. 3. (a) Temperature dependence of magnetic susceptibility (χ) in $(Ce_{1-x}Nd_x)_3Al$ from 2 to 300 K at an external field of $H=1$ kOe. (b) Fit of the Rajan's curve (solid lines) to the experimental result of the magnetic susceptibility, making T_0 as a fitting parameter (see text) (Ref. 25).

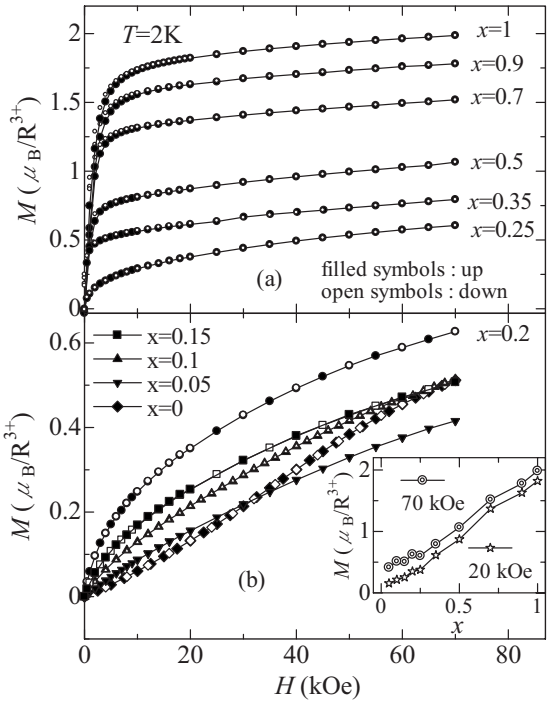

FIG. 4. Magnetic field dependence of magnetization for $(Ce_{1-x}Nd_x)_3Al$ at 2 K with increasing and decreasing field. The inset shows the magnetic moment at 2 K under 20 and 70 Oe as function of x in $(Ce_{1-x}Nd_x)_3Al$.

According to the Bethe-Ansatz solution of the Coqblin-Schrieffer model, the physical properties of a Kondo lattice are well scaled by a single energy parameter (T_0).[24,25] We estimate the characteristic temperatures for $x=0$, 0.05, and 0.1 by using Rajan's numerical results.[25] As shown in Fig. 3(b), we fit the Rajan's curve to the experimental result of the magnetic susceptibility, making T_0 and $\chi(0)$ as fitting parameters. Note that we assumed the total angular momentum of $J=1/2$ instead of $J=5/2$ by taking into account the crystal-field effect. T_0 is estimated to be about 5.9, 2.3, and 1.6 K for $x=0$, 0.05, and 0.1, respectively.

Figure 4 shows the magnetization curves $M(H)$ measured at 2 K up to 70 kOe. The magnetization tends to be saturated at low field for Nd-rich samples. An almost linear increase in the magnetization with increasing magnetic field was found for Ce-rich samples. The magnetization at 2 K under 20 and 70 kOe as a function of x is shown in the inset of Fig. 4(b). The difference between 20 and 70 kOe decreases gradually with increasing x. These behaviors indicate that at low temperature the AFM contribution is larger for Ce-rich samples, in contrast, the FM is dominant for Nd-rich samples. These characters are consistent with the magnetization measurement as a function of temperature as shown below.

The temperature dependence of reciprocal susceptibility $(1/\chi)$ at 1 kOe are shown in Fig. 5. The anomalous change around 110 K for Ce-rich sample is due to the crystal phase transition which is confirmed by low-temperature XRD.[26] The reciprocal susceptibility in the high-temperature region could be described by the Curie-Weiss law, i.e., $\chi=C/T-\Theta_p$, where C is the curie constant and Θ_p is the paramagnetic Curie temperature.

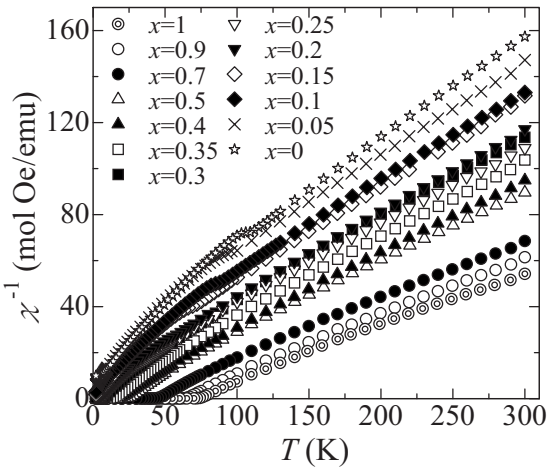

FIG. 5. Temperature dependence of inverse magnetic susceptibility $(1/\chi)$ at 1 kOe in $(Ce_{1-x}Nd_x)_3Al$.

The effective magnetic moments, μ_{eff}, and the paramagnetic Curie temperature, Θ_p, as a function of x deduced from the Curie-Weiss law are shown in Fig. 6. The values of μ_{eff} and Θ_p gradually increase with the decreasing x. Θ_p is negative for Ce-rich samples but positive for Nd-rich ones, i.e., the magnetic transition is transferred from AFM to FM with the increase in Nd concentration. The estimated value of μ_{eff} for Ce_3Al and Nd_3Al are $2.49\mu_B$ and $3.56\mu_B$, which are close to the values of free ions; Ce^{3+} $(2.54\mu_B)$ and Nd^{3+} $(3.62\mu_B)$, respectively. Indeed, the experimentally derived values of μ_{eff} are consistent with those of theoretical calculated by the equation $\mu_{eff}=[(1-x)[\mu_{eff}(Ce^{3+})]^2+x[\mu_{eff}(Nd^{3+})]^2]^{1/2}$. This result indicates that the electronic structures of Nd and Ce ions in the ground states do not have a pronounced change in the entire range for $(Ce_{1-x}Nd_x)_3Al$ system. Negative Curie temperature, however, implies possible hybridization of the Ce $4f$ electrons with the conduction electrons as well as antiferromagnetic correlation between Ce moments for Ce-rich samples.

Figure 7 shows the temperature dependence of normalized electrical resistivity $\rho(T)/\rho(300\ \mathrm{K})$ for both cases with

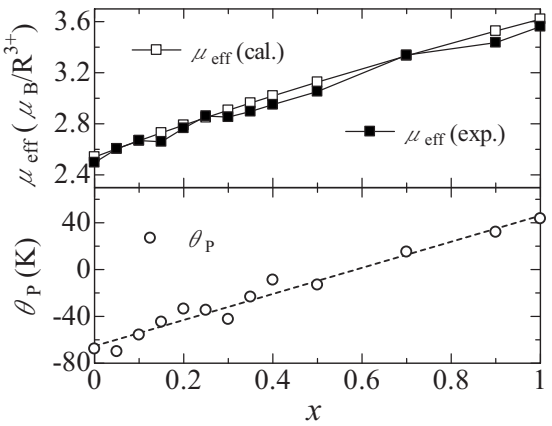

FIG. 6. The values of experimentally derived (closed square) and theoretically calculated (open square) effective magnetic moments, μ_{eff}, as well as the paramagnetic Curie temperature (open circle), Θ_p, as a function of x in $(Ce_{1-x}Nd_x)_3Al$.

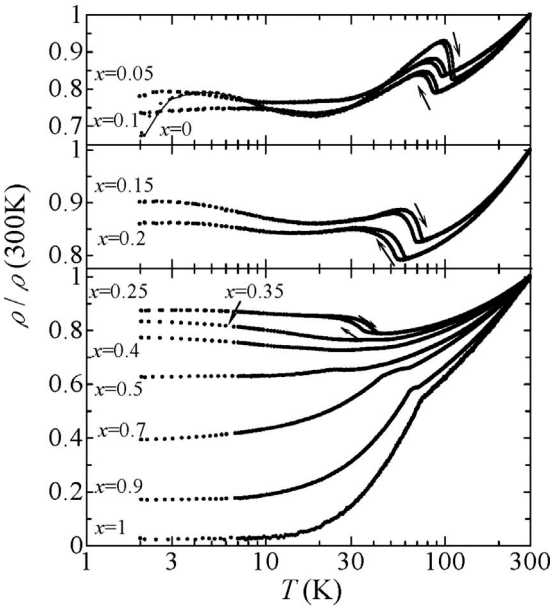

FIG. 7. Temperature dependence of normalized electrical resistivity $\rho(T)/\rho(300\ \mathrm{K})$ with increasing and decreasing temperature in $(Ce_{1-x}Nd_x)_3Al$ at the temperature range between 2 and 300 K.

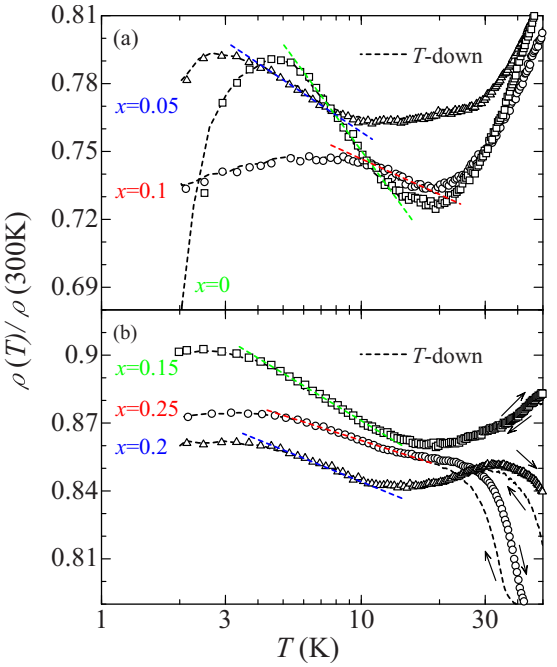

FIG. 8. (Color online) Low-temperature log T dependence of normalized resistivity $\rho(T)/\rho(300\ \mathrm{K})$ at $x \leq 0.30$ in $(Ce_{1-x}Nd_x)_3Al$. Straight lines are guide for the eyes.

increasing and decreasing temperature between 2 and 300 K. For the Ce_3Al and Ce-rich samples, an obvious hysteresis can be seen, which is attributed to a crystal phase transition from hexagonal to monoclinic and these transitions are confirmed by low-temperature XRD.[26] A change in slope is observed in Nd-rich samples with decreasing temperature, corresponding to the magnetic transition temperature, T_C, from PM to FM. The crystal structure transition temperature, T_S, decreases rapidly with increasing Nd concentration, and vanishes for $x > 0.35$, which is consistent with the temperature dependence of the crystal structure study.[26] There is a clear upturn in resistivity after structure phase transition. The high-temperature resistivity (above T_C or T_S) shows an almost linear temperature dependence for all the samples. We show the low-temperature log T dependence of normalized resistivity for $x < 0.30$ in Fig. 8. The log T dependence of the resistivity has the minimum and linear parts, suggesting clear evidence of the single-impurity Kondo region. The Kondo effect is only observed in the Ce-rich samples and disappears rapidly with increasing Nd concentration. The peak at low temperature is due to the antiferromagnetic order in Ce-rich samples and possible coherence effect.[17,23] For Ce-rich samples we observe the Kondo effect in the resistivity measurement and as will be shown later the system shows large electronic specific-heat coefficient. These results suggest that we could expect Fermi-liquid behavior for Ce-rich samples but at $T \geq 2$ K we do not observe the T^2 dependence for the resistivity. In $YbCu_{5-x}Al_x$ T^2 and $\log(T)$ dependences were observed at low and intermediate temperature regions, respectively.[27] The region where T^2 dependence was seen corresponded to the temperature region below the maximum temperature (T_m) in χ-T curve. In Ce-rich cases of our system the Kondo temperature and T_m are the order of a few K and thus the Fermi-liquid behavior with Kondo lattice formation may be observable at much lower temperature than a few K, which is beyond the measured temperature range.

The temperature dependence of specific heat $[C(T)]$ per formula unit of $(Ce_{1-x}Nd_x)_3Al$ is shown in Fig. 9. A λ-shape behavior near T_C for Nd-rich samples and peaks at low temperatures for Ce-rich samples in $C(T)$ are believed to be due to the magnetic structure transition which is confirmed by the

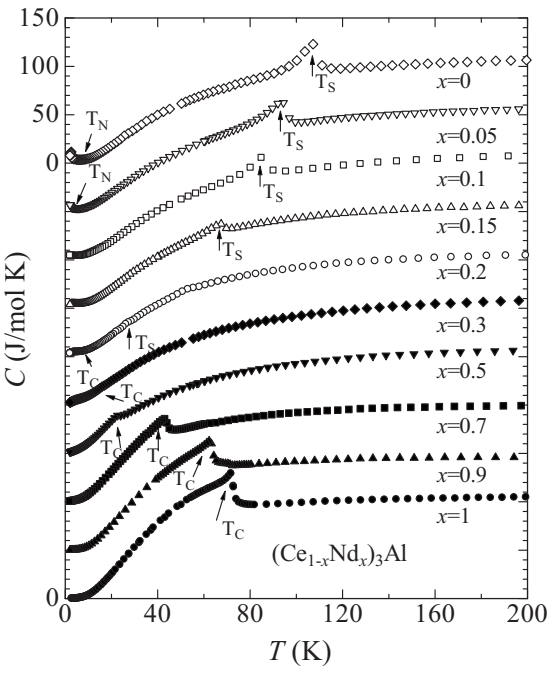

FIG. 9. Temperature dependence of specific heat (C) per formula unit in $(Ce_{1-x}Nd_x)_3Al$. T_S, T_N, and T_C are structural transition temperature, Néel temperature, and Curie temperature, respectively.

TABLE I. The volume (V), Curie constant (C), Debye temperature (Θ_D), Curie temperature (T_C), structural transition temperature (T_S), and Néel temperature (T_N) as a function of x in $(Ce_{1-x}Nd_x)_3Al$ ($x=0-1.0$) system. T_0 is the characteristic temperature obtained by the fitting of Rajan's curve for $J=1/2$ (Ref. 25).

x	V (Å^3)	C (emu K/mol)	Θ_D (K)	T_C (K)	T_S (K)	T_N (K)	T_0 (K)
0	233.62	2.34	171		105	2.9	5.9
0.05	233.06	2.54	170		87	2.3	2.3
0.1	232.63	2.67	196		81		1.6
0.15	232.47	2.65	177	4	60		
0.2	232.64	2.87	176	5	44.5		
0.3	231.48	3.01	177	7	24.5		
0.5	231.83	3.49	137	24			
0.7	231.35	4.18	117	45			
0.9	230.00	4.43	149	65			
1.0	229.60	4.76	157	74			

magnetization measurement. There is also an obvious peak in $C(T)$ around the crystal phase-transition temperature T_S at $x \leq 0.3$. The results of T_C, T_N. and T_s as well as some other parameters for $(Ce_{1-x}Nd_x)_3Al$ system are summarized in Table I.

Medina *et al.*[16] discussed the relation between the unit-cell volume and T_K in Kondo system $(Ce_{1-x}La_x)_3Al$. They used the relation for the change in T_K; $T_K = T_K(Ce_3Al)\exp(\{1-\exp[q(V-V_0)/V_0]\}/|\rho J|_0)$, where q, V, ρ, and J are a parameter between 6 and 8, volume, density of state (DOS), and Kondo exchange parameter, respectively. They showed that $|\rho J|_0$ decreases as decreasing x. Thus as increasing La concentration, both the DOS and T_K decrease. Ion radius of La^{3+} is larger than that of Ce^{3+}. Therefore increase in La concentration corresponds to the increase in the volume as described before. This may result the decrease in the Ce c-f hybridization and the Kondo temperature. Thus in $(Ce_{1-x}La_x)_3Al$ the enhancement of T_K with decreasing Ce concentration x, corresponding to the volume contraction, is related to the reduction in T_N due to the competition between the Kondo effect and RKKY interaction. In $(Ce_{1-x}Nd_x)_3Al$ as increasing the Nd concentration we observe the decrease in the volume, but ΔV is very small, especially in the region $x \leq 0.2$, where the Kondo effect is observed. Nd substitution to Ce site, however, causes the strong decrease in T_0 as well as T_N, may be due to the existence of Nd f electrons, in contrast to the lack of f electron in La^{3+} ions in $(Ce_{1-x}La_x)_3Al$. Thus we cannot apply above equation for $(Ce_{1-x}Nd_x)_3Al$ system. The reduction in T_0 and T_N is originated by the increase in the ferromagnetic local-moment character with the increase in a small Nd concentration. A possible scenario is that Nd substitution may cause the narrowing and increase in the DOS and a shift of the Fermi level as observed in Lu-doped Yb compounds.[28,29] This anomaly due to Nd substitution to Ce site in Ce_3Al will be also discussed in the electronic-structure measurements by x-ray spectroscopic methods.[26]

IV. CONCLUSION

As a summary of the crystal structure, electronic, magnetic, and thermodynamic study results, we present the crystal and magnetic phase diagram of the $(Ce_{1-x}Nd_x)_3Al$ system in Fig. 10. In $(Ce_{1-x}Nd_x)_3Al$ we could observe the phase transition clearly from the Kondo system to magnetic ordered state. The crystal phase transition is confirmed for $x \leq 0.35$ similar to that of Ce_3Al, and the transition temperature decreases with increasing x. Ce rich and Ce_3Al show antiferromagnetic phase transition, and T_N decreases with increasing x. Nd_3Al and Nd-rich samples are ferromagnetic and the Curie temperature T_C increases gradually with increasing x at $x \geq 0.2$. The resistivity measurement shows the evidence of the Kondo effect for Ce-rich samples. The order of the estimated characteristic temperatures from the fit with

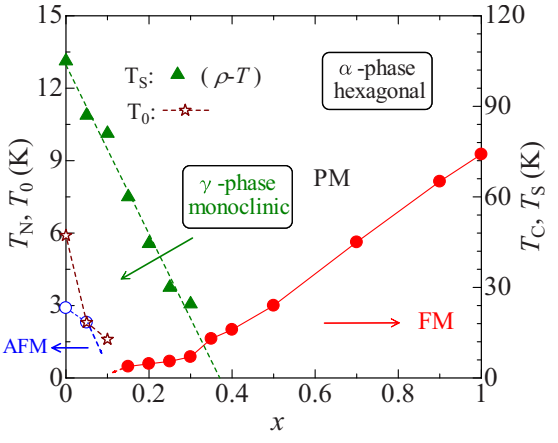

FIG. 10. (Color online) Phase diagram of $(Ce_{1-x}Nd_x)_3Al$ system. T_C (closed circle), T_S (closed triangle), T_N (open circle), and T_0 (star) correspond to magnetic transition temperature from paramagnet to ferromagnet, structural transition temperature, Néel temperature, and characteristic temperature obtained by the fitting of Rajan's curve, respectively.

the solution of the Coqblin-Schrieffer decreases rapidly with increasing Nd concentration as well as the Neél temperature. In Ce_3Al as decreasing the temperature the Kondo effect is dominant after the structural transition and magnetic phase transition from PM to FM occurs. A small Nd substitution to Ce site dilutes the Kondo effect strongly and around $x \sim 0.2$ the Kondo effect disappears. At low temperature $x \sim 0.2$ is the critical point of the two competing interactions of ferromagnetic ordered state and Kondo effect and $x \sim 0.1$ may be the point where the AFM order disappears. Interestingly the structural transition temperature T_S crossovers with the magnetic transition temperature T_C around $x = 0.35$ at low temperature, showing that the structural transition is less effective on the electronic state in this temperature and x ranges. In contrast to the result for $(Ce_{1-x}La_x)_3Al$, our measurements for $(Ce_{1-x}Nd_x)_3Al$ show that the Kondo temperature increases with the slight increase in the volume, indicating anomaly due to the Nd content.

ACKNOWLEDGMENT

This work was supported by a Grant in Aid for Scientific Research No. 19740221 from Ministry of Education, Culture, Sports, Science and Technology of Japan.

[1] E. A. Goremychkin, R. Osborn, B. D. Rainford, T. A. Costi, A. P. Murani, C. A. Scott, and P. J. C. King, Phys. Rev. Lett. **89**, 147201 (2002).
[2] Y. Nishida, A. Tsuruta, and K. Miyake, J. Phys. Soc. Jpn. **75**, 064706 (2006).
[3] S. Raj, Y. Iida, S. Souma, T. Sato, T. Takahashi, H. Ding, S. Ohara, T. Hayakawa, G. F. Chen, I. Sakamoto, and H. Harima, Phys. Rev. B **71**, 224516 (2005).
[4] N. N. Tiden, P. A. Alekseev, V. N. Lazukov, A. Podlesnyak, E. S. Clementyev, and A. Furrer, Solid State Commun. **141**, 474 (2007).
[5] H. Ikeda, J. Phys. Soc. Jpn. **71**, 1126 (2002).
[6] H. H. Cho, W. H. Lee, and Y. Y. Chen, Solid State Commun. **130**, 821 (2004).
[7] T. Nakano, K. Sengupta, S. Rayaprol, M. Hedo, Y. Uwatoko, and E. V. Sampathkumaran, J. Phys.: Condens. Matter **19**, 326205 (2007).
[8] G. R. Stewart, Rev. Mod. Phys. **56**, 755 (1984).
[9] N. B. Brandt and V. V. Moshchalkov, Adv. Phys. **33**, 373 (1984).
[10] K. H. J. Buschow and J. H. N. van Vucht, Z. Metallkd. **57**, 162 (1966).
[11] K. Okuda, S. Noguchi, Y. Takigawa, Y. Murashita, J. Sakurai, and H. Fujii, J. Phys. Soc. Jpn. **58**, 2630 (1989).
[12] J. Sakurai, Y. Murashita, Y. Aoki, T. Fujita, T. Takabatake, and H. Fujii, J. Phys. Soc. Jpn. **58**, 4078 (1989).
[13] T. Kagayama and G. Oomi, J. Phys. Soc. Jpn. **65**, 42 (1996).
[14] L. S. Azechi, A. N. Medina, and F. G. Gandra, J. Appl. Phys. **81**, 4179 (1997).
[15] Y. Y. Chen, J. M. Lawrence, J. D. Thompson, and J. O. Willis, Phys. Rev. B **40**, 10766 (1989).
[16] A. N. Medina, M. A. Hayashi, L. P. Cardoso, S. Gama, and F. G. Gandra, Phys. Rev. B **57**, 5900 (1998).
[17] Y. Y. Chen, Y. D. Yao, B. C. Hu, C. H. Jang, J. M. Lawrence, H. Huang, and W. H. Li, Phys. Rev. B **55**, 5937 (1997).
[18] Q.-S. Zeng, Y. Ding, W. L. Mao, W. Luo, A. Blomqvist, R. Ahuja, W. Yang, J. Shu, S. V. Sinogekin, Y. Meng, D. L. Brewe, J.-Z. Jiang, and H.-k. Mao, Proc. Natl. Acad. Sci. U.S.A. **106**, 2515 (2009).
[19] Y. Y. Chen, Y. D. Yao, C. R. Wang, W. H. Li, C. L. Chang, T. K. Lee, T. M. Hong, J. C. Ho, and S. F. Pan, Phys. Rev. Lett. **84**, 4990 (2000).
[20] T. F. Smith and H. L. Luo, J. Phys. Chem. Solids **28**, 569 (1967).
[21] T. Sakurai, Y. Murashita, H. Fujiwara, H. Kadomatsu, I. Oguro, and J. Sakurai, J. Magn. Magn. Mater. **115**, 250 (1992).
[22] T. Fukuhara, R. Yamagata, L. Li, K. Nishimura, and K. Maezawa, J. Phys. Soc. Jpn. **78**, 034723 (2009).
[23] C. S. Garde, J. Ray, and G. Chandra, J. Phys.: Condens. Matter **1**, 2737 (1989).
[24] B. Coqblin and J. R. Schrieffer, Phys. Rev. **185**, 847 (1969).
[25] V. T. Rajan, Phys. Rev. Lett. **51**, 308 (1983).
[26] H. Yamaoka, I. Jarrige, R. Yamagata, K. Nishimura, N. Hiraoka, H. Ishii, and K.-D. Tsuei (unpublished).
[27] K. Yoshimura, N. Tsujii, J. He, and K. Kosuge, Jpn. J. Appl. Phys. Part 1 **8**, 363 (1999).
[28] T. Susaki, T. Konishi, A. Sekiyama, T. Mizokawa, A. Fujimori, T. Iwasaki, S. Ueda, T. Matsushita, S. Suga, H. Ishii, F. Iga, and M. Kasaya, Phys. Rev. B **56**, 13727 (1997).
[29] J. Yamaguchi, A. Sekiyama, S. Imada, A. Yamasaki, M. Tsunekawa, T. Muro, T. Ebihara, Y. Onuki, and S. Suga, New J. Phys. **9**, 317 (2007).